



## Analysis of noise in differential and ratiometric biosensing systems

Sidahmed A. Abayzeed<sup>a,\*</sup>, Richard J. Smith<sup>a</sup>, Chung W. See<sup>a</sup>, Michael G. Somekh<sup>b</sup>

<sup>a</sup> Optics and Photonics Research Group, Faculty of Engineering, University of Nottingham, Nottingham NG7 2RD, UK

<sup>b</sup> Electronic and Information Engineering, The Hong Kong Polytechnic University, Hung Hom, Kowloon, Hong Kong, China



### ARTICLE INFO

#### Article history:

Received 24 June 2017

Received in revised form

14 December 2017

Accepted 2 January 2018

Available online 3 January 2018

#### Keywords:

Differential or ratiometric measurements

Surface plasmon resonance sensors

Biosensing

Chemical sensors

### ABSTRACT

This paper presents formulations to evaluate noise in differential and ratiometric measurements that are often performed in biosensing. These measurements are performed to improve signal to noise ratio of the sensing systems for sensitive detection of dynamic biological processes. The use of these formulations is discussed in the context of the differential intensity surface plasmon resonance (SPR) system that is widely used to characterise molecular interactions on a confined axial scale. Previous studies provide qualitative descriptions of the noise performance of such systems but lack rigorous characterisation. Here we present analytical expressions for quantitative evaluation of the noise in differential and ratiometric measurements by applying the rules of arithmetic operations on random variables. Such formulations provide the means for evaluating the signal to noise ratio of such systems. We present how correlated noise can be removed by performing differential or ratiometric processing. Applying these formulations, we also show how the sensitivity of the differential intensity SPR system changes during the experiment.

© 2018 The Author(s). Published by Elsevier B.V. This is an open access article under the CC BY license (<http://creativecommons.org/licenses/by/4.0/>).

## 1. Introduction

Differential or ratiometric processing is often employed to enhance the signal to noise ratio or the sensitivity of biosensing systems. It is driven by the demand to develop highly sensitive instruments capable of resolving small signals related to biological processes. In this study, we present an analytical approach to evaluate noise in differential and ratiometric measurements. The proposed method is discussed in the context of noise in differential intensity surface plasmon resonance (DI-SPR) instrument. For instance, differential measurements are performed in surface plasmon resonance (SPR) sensors that uses bicell detectors [1]. SPR sensors utilise the properties of propagating surface plasmons at a noble metal-dielectric interface. Surface plasmons are excited with p-polarised light that matches their wavevector, which is commonly achieved by using Kretschmann-Raether configuration [2]. In this configuration, the excitation of surface plasmons features a minimum in the intensity of the reflected light [3] in addition to a sharp change of its phase [3]. This resonance position is sensitive to the optical properties of both the metal and the dielectric material which provides mechanisms for detecting small changes within the sample in the close proximity to the metal surface [4] or change in electron density within the metal surface [5]. For instance, refrac-

tive index changes typically between  $1 \times 10^{-7}$ – $1 \times 10^{-5}$  refractive index units (RIUs) [6] are detected within the evanescent field depth (of the order of 100 nm).

Different detection schemes and optical configurations are used to design SPR systems [7], based on measurement of the intensity [8], the phase [9] of the reflected light at a specific angle of incidence or tracking the resonance angle [10] or the resonance wavelength [11]. For instance, in differential intensity SPR systems [1,12], SPs are excited by focusing light, coupled through a prism, onto the gold surface. The reflected light is detected by a bicell photodiode whose outputs ( $A$  and  $B$ ) are processed to compute the difference to sum ratio  $(A - B)/(A + B)$ . The detector is initially balanced to obtain the maximum sensitivity [13]. Shifting from this detector position, with respect to the resonance curve, is directly related to the change in refractive index of the sample [13].

Previous work was directed at understanding the factors that affect the response of the system to change in refractive index [13], however, the noise performance of the system still requires further clarification. This paper, therefore, presents a method for calculating noise of such systems by utilising the rules of arithmetic operations on random variables [14,15]. Moreover, differential approaches were used in other plasmonic systems that includes nanohole arrays based systems [16] or low noise SPR systems [17,18], which can benefit from our approach to noise calculations. It is worth mentioning that differential approaches are not only used in intensity measurements, but they are also used in phase based SPR systems [19,20]; Wu et al [20] demonstrated that dif-

\* Corresponding author.

E-mail address: [sidahmed.abayzeed@nottingham.ac.uk](mailto:sidahmed.abayzeed@nottingham.ac.uk) (S.A. Abayzeed).

ferential phase between s and p polarised light can be performed, using a dual interferometers (i.e. for reference and sensing), to increase the sensitivity of phase based systems.

Characterising the noise of a sensing system is crucial as it sets its limit of detection. Sources of noise in SPR measurements are discussed in the literature [21,22]. It includes relative intensity noise [22] that is described as fluctuations in the laser intensity, shot noise due to the quantum arrival of photons at the detector and the readout noise from the detector and the electronics [22]. When multiple detection channels are used, the correlation or its absence plays a crucial role in the overall noise performance of the system. Indeed carefully accounting for the noise correlations in different channels provides a route to signal to noise ratio optimisation as demonstrated for structured illumination microscopy in [23].

One of the sources of correlated noise is laser fluctuations, in reality the detection limit of most of the intensity SPR systems is degraded by this noise [22] and shot-noise limited detection is not often achievable. Also, quantitative analysis for evaluating the removal of correlated noise is lacking. For the case of the bicell detection, the correlation between the dynamic signals on both units of the detector is of a particular importance, since both difference and division are performed on the detected signals. Here, we present analytical expressions to estimate the noise in the presence of various degrees of correlations between signal channels comparing the effect of both differential and ratiometric processing. This analysis can be applied beyond SPR systems since bicell or quadrant detectors are also used in interferometry [24], position sensing [25], dynamic edge detection [26] or laser acoustic systems [27]. Additionally, it can be applied to systems that use ratiometric processing such as ratiometric calcium sensing [28] or modulation depth measurements [29]. In Section 2 of this paper, we provide description of theory of noise in differential and ratiometric measurements. In Sections 3 and 4 we describe experiments and results characterising the noise in differential intensity surface plasmon resonance, as an example for practical applications.

## 2. Theory

Temporal fluctuations of a system response can be represented with a random variable and the associated noise is found from the standard deviation of these fluctuations. When mathematical operations such as difference or division are performed, the resulting noise can be found from the variance of this derived quantity. Estimating the noise is essential to the characterisation of the overall signal to noise ratio of the system. This involves calculation of the variance of sums, differences and ratios as described in standard texts [14,15]. In the following paragraphs, total noise after difference, sum or division is described for the case of using bicell detectors.

### 2.1. Differential and ratiometric noise

The variance of the difference or the sum of two signals A and B can be found from [14]

$$\sigma_{A \pm B}^2 = \sigma_A^2 + \sigma_B^2 \pm 2\text{cov}(A, B) \quad (1)$$

The covariance of the two signals  $\text{cov}(A, B)$  can be expressed as a function of the correlation between the two signals [15] as

$$\text{cov}(A, B) = \sigma_A \sigma_B \text{corr}(A, B) \quad (2)$$

Eq. (1) can therefore be rewritten in terms of correlation as

$$\sigma_{A \pm B}^2 = \sigma_A^2 + \sigma_B^2 \pm 2\sigma_A \sigma_B \text{corr}(A, B) \quad (3)$$

It is worthwhile mentioning that Eq. (3) is analogous to the cosine rule and can be represented by the phasor diagram in Fig. 1

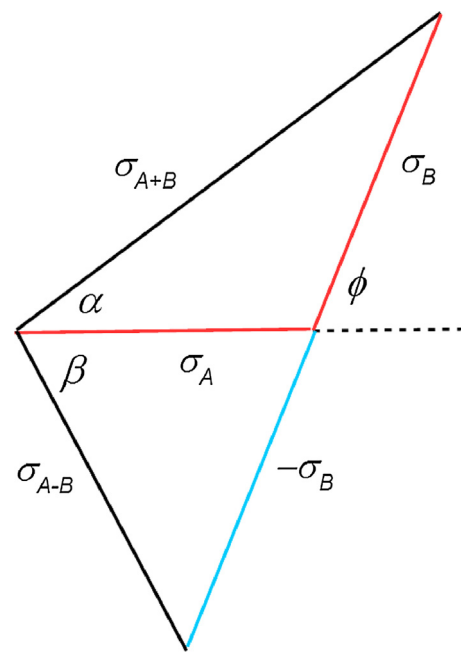


**Fig. 1.** Phasor diagram shows the difference and sum of two noise components which are represented by the standard deviation ( $\sigma_A$  and  $\sigma_B$ ) with a phase angle  $\phi$  whose cosine equals to the correlation between the signals A and B. It is obvious from the graph that the difference ( $A - B$ ) and the sum ( $A + B$ ) are uncorrelated when the variances of A and B are equal.

where  $\text{corr}(A, B)$  is equivalent to the cosine of the angle ( $\phi$ ) between the vectors  $\sigma_A$  and  $\sigma_B$ . The geometrical representation of noise in differential and ratiometric processing is useful to study the effect of the correlation between the signals as will be explained later in Section 2.2.

The variance of the ratio of two signals (N and D) is more complex; in addition to the variance of each one of the two signals, it also depends on the average of each of the two signals and the correlation between them. The general form is

$$\sigma_{\frac{N}{D}}^2 \approx \frac{\mu_D^2 \sigma_N^2 + \mu_N^2 \sigma_D^2 - 2\text{cov}(N, D)\mu_N \mu_D}{\mu_D^4} \quad (4)$$

This equation is presented in [15] and derived from a first order Taylor expansion in [30] under the condition that the denominator takes values  $[0, \infty)$ . In order to explore the conditions that affect the accuracy of this equation, we calculated the standard deviation of the ratio of two signals using this equation taking into consideration the ratio of the mean to the standard deviation of both the numerator and the denominator in addition to the correlation between them. For this purpose, two signals (i.e. numerator and denominator) with Rician distributions were generated using Monte Carlo simulations, averaged over  $10^4$  points. The ratio of the mean to the standard deviation of numerator is varied between  $-10$  and  $10$  while the ratio of the mean to the standard deviation of the denominator is varied for values from  $0$  to  $200$ . Normalised percentage error is obtained from the standard deviation estimated using Eq. (4) compared to the directly calculated standard deviation.

As observed in Fig. 2(a), the error of this expansion is dominated by the ratio of the mean to standard deviation of the denominator and is also a weak function of the correlation between the numerator and the denominator. It is reduced by increasing this ratio and it becomes  $<3\%$  for ratios  $>20$  (see Fig. 2(b)) that are a lot smaller than the ratio in a typical experiment. Generally, the denominator is used for referenced measurements and usually not affected by the measured quantity. By ensuring sufficient signal to noise ratio ( $>20$ ) for the denominator channel, the expression in Eq. (4) can

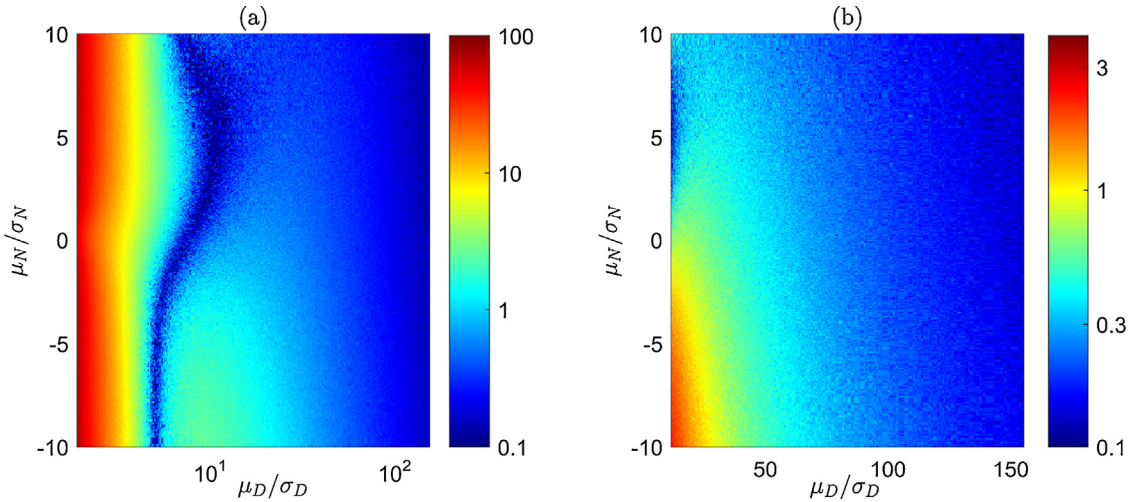


**Fig. 2.** Accuracy in the estimation of the noise of the ratio using Eq. (4). Accuracy is presented by normalised percentage error in (a) that is calculated from the difference between the standard deviation obtained by Eq. (4) and the directly calculated standard deviation. The error map is shown for  $\mu_D/\sigma_D > 10$  in (b). The maps are calculated for a correlation of 0.5 and similar response is obtained for other correlations (data not shown).

be used to accurately predict the noise of the ratio. The use of this expression to evaluate the noise in bicell detector based SPR system is discussed in Section 4.3. Eq. (4) can be also re-arranged to the form that is analogous to the cosine rule [31] as

$$\left(\frac{\sigma_{N/D}}{\mu_{N/D}}\right)^2 = \left(\frac{\sigma_N}{\mu_N}\right)^2 + \left(\frac{\sigma_D}{\mu_D}\right)^2 - 2 \left(\frac{\sigma_N}{\mu_N}\right) \left(\frac{\sigma_D}{\mu_D}\right) \text{corr}(D, N) \quad (5)$$

The form of Eq. (5) provides a convenient way to understand the noise to signal ratio (NSR) of the division of two signals taking into consideration the NSR of both the numerator and the denominator in addition to the correlation between them. This equation brings out similarities to subtraction by taking the form of the cosine rule. The main difference is that the division is expressed in terms of noise to signal ratio rather than the noise above.

As can be seen from Eqs. (4) and (5), the correlation between the signals in the differential and ratiometric measurements plays an important role. In order to study its effect, two signals  $s_1 = ax + bz$ ,  $s_2 = ay + bz$  were generated by Monte Carlo simulations using various weighted combinations of uncorrelated random ( $x, y$ ) and correlated noise ( $z$ ). The correlated noise is varied relative to random noise in order to design different correlations between the two signals. Average values and standard deviations were calculated over  $10^4$  points. As observed in Fig. 3(a), this correlated noise component is removed by taking the difference of the two signals and the noise increases when the summing is performed as expected. Similarly, performing the division leads to the same result of the difference as presented in Fig. 3(b). Since the ratio and the difference are on different scales, the comparison is presented in terms of the noise to signal ratio. Fig. 3(b) confirms the analogy between the difference and the division in the removal of the correlated component of the noise.

## 2.2. Noise of normalised differential signals

In optical sensing systems that use bicell detectors [1,24], the output of the system is obtained by taking the ratio of the difference and the sum of the two channels of the bicell. Compared to performing referenced measurements with a single photodetector, the bicell outputs are common path signals and therefore is expected to provide a better cancellation of the correlated noise. As mentioned earlier, the differencing and summing affect the correlation between the numerator and the denominator. In this section, we discuss how these factors combine to affect the noise performance.

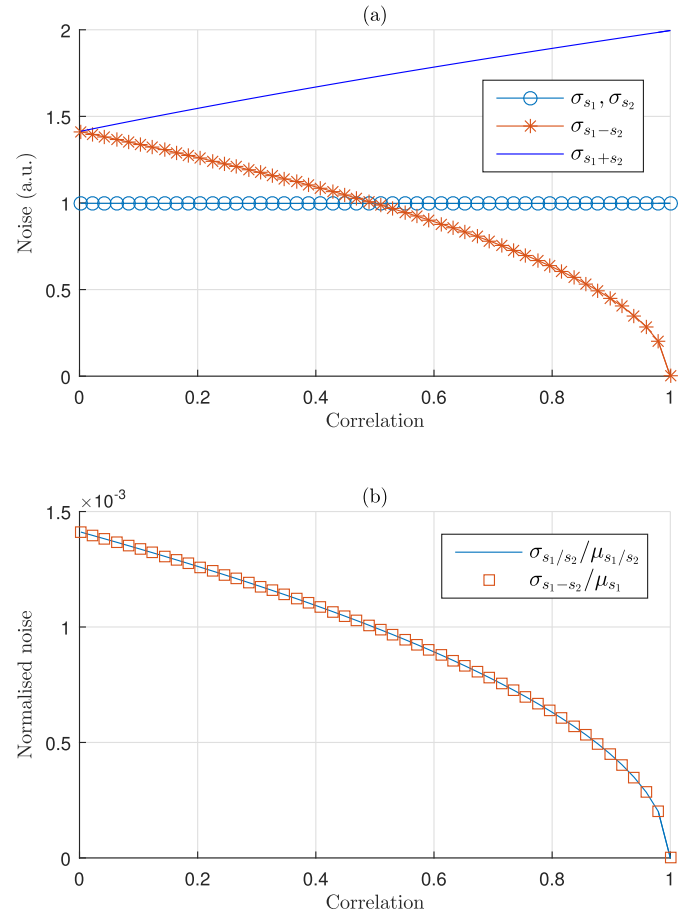


**Fig. 3.** The removal of correlated noise in ratiometric or differential measurements. Two signals  $s_1$  and  $s_2$  with equal noise values are presented by circles in (a); the correlation between  $s_1 = ax + bz$  and  $s_2 = ay + bz$  was simulated in the range (0–1) by setting  $a = \sqrt{n}$  where  $n = 1, \dots, 0$  and  $b = \sqrt{1 - n}$ . The effect of the difference (\*) and the sum (solid line) is presented. (b) A comparison between the noise of the ratio and the noise of the difference normalised to the average of the ratio and the average of the signal  $s_1$  respectively.

In order to estimate the noise of the ratio, one needs to know the average value and the noise of both the difference and the sum, in

addition to their covariance as shown in Eq. (6).

$$\sigma_T^2 = \frac{\mu_{(A+B)}^2 \sigma_{(A-B)}^2 + \mu_{(A-B)}^2 \sigma_{(A+B)}^2 - 2\text{cov}(A-B, A+B)\mu_{(A-B)}\mu_{(A+B)}}{\mu_{(A+B)}^4} \quad (6)$$

The noise of the difference or the sum can be found from Eq. (1) while the covariance between the signals  $(A-B)$  and  $(A+B)$  can be found from the geometry in Fig. 1 in the following two steps

$$\text{corr}(A-B, A+B) = \cos(\alpha + \beta) = \left( \frac{\sigma_A^2 - \sigma_B^2}{\sigma_{A+B}\sigma_{A-B}} \right) \quad (7)$$

Similar to Eq. (2), the covariance can be found with the knowledge of the correlation as

$$\text{cov}(A-B, A+B) = \sigma_A^2 - \sigma_B^2 \quad (8)$$

The noise of the ratio  $(A-B)/(A+B)$  can be re-written as

$$\sigma_T^2 = \frac{\mu_{(A+B)}^2 \sigma_{(A-B)}^2 + \mu_{(A-B)}^2 \sigma_{(A+B)}^2 - 2\mu_{(A-B)}\mu_{(A+B)}(\sigma_A^2 - \sigma_B^2)}{\mu_{(A+B)}^4} \quad (9)$$

Under the condition that the detector is balanced, the covariance between  $(A-B)$  and  $(A+B)$  becomes zero, similarly the mean of  $(A-B)$  approaches zero and thus Eq. (9) reduces to

$$\sigma_T = \frac{\sigma_{(A-B)}}{\mu_{(A+B)}} \quad (10)$$

As discussed later in Section 4, these sets of equations can be used to estimate the noise to signal ratio of SPR systems that use bicell detectors. They suggest that when the detector is unbalanced, the noise of  $(A-B)/(A+B)$  does not only depend on the noise of difference and the sum but also their average values. These predictions will be confirmed experimentally in Section 4.4. However for a balanced detector, noise of the ratio is related to the reciprocal of the sum of the bicell channels, and therefore can be reduced by increasing the total detected power.

### 2.3. Comparison between differential and ratiometric processing in canceling multiplicative noise

So far we considered how correlated noise can be removed using differential and ratiometric processing. However, the nature of noise (i.e. additive or multiplicative) has not been discussed. In this section, we provide a comparison between the differential and ratiometric processing in the removal of the correlated multiplicative noise (e.g. laser fluctuations). Let us consider the case where measurements are over a timescale with significant laser fluctuation that does not average out. Considering a measurement system where a bicell detector with channels  $A$  and  $B$  is used. Let  $P_A$  and  $P_B$  be fractions of the incident power where ( $P_A + P_B = 1$ ) and  $\Delta P = P_A - P_B$ . Using a laser power of  $(I + \delta I)$ , the difference and the sum are given by:

$$A - B = (I + \delta I)\Delta P + n_A - n_B \quad (11)$$

$$A + B = (I + \delta I) + n_A + n_B \quad (12)$$

where  $n_A$  and  $n_B$  are random noise from the detector channels  $A$  and  $B$ . The difference  $(A - B)$  contains both additive and multiplicative noise. For a balanced detector or a nearly balanced detector, multiplicative noise is canceled as ( $\Delta P \rightarrow 0$ ) and the additive noise dominates. Now let us consider the ratiometric approach, starting with  $A = (I + \delta I)P_A + n_A$  and  $B = (I + \delta I)P_B + n_B$ , the ratio of  $(A/B)$  is:

$$\frac{A}{B} = \frac{P_A \left( 1 + \frac{\delta I}{I} \right) + \frac{n_A}{IP_B}}{1 + \frac{\delta I}{I} + \frac{n_B}{IP_B}} = \frac{P_A}{P_B} + \frac{P_B n_A - P_A n_B}{IP_B^2} \quad (13)$$

After multiplying by the term  $(1 - \frac{\delta I}{I} - \frac{n_B}{IP_B})$  and retaining the first order and under the assumption that  $\delta I/I, n_B/IP_B \ll 1$ , the multiplicative term  $\delta I/I$  will be removed even if the detector is unbalanced (i.e.  $P_A/P_B \neq 1$ ), in contrast to the difference where the multiplicative term is only removed if the detector is nearly balanced. The same analysis can be applied to the case of the ratio of  $(A - B)/(A + B)$  as shown in Eq. (14). When the detector is unbalanced,  $(\Delta P \neq 0)$  and therefore the additive random noise dominates and scales with the average value of both the numerator and the denominator. This observation is confirmed experimentally in Section 4.4 where its implications on the sensitivity of the sensing is also discussed.

$$\frac{A - B}{A + B} = \frac{\Delta P \left( 1 + \frac{\delta I}{I} \right) + \frac{n_A - n_B}{I}}{1 + \frac{\delta I}{I} + \frac{n_A + n_B}{I}} = \Delta P + \frac{n_A - n_B - \Delta P(n_A + n_B)}{I} \quad (14)$$

Similar to bicell detector based systems, the removal of the correlated multiplicative noise is important for measurements performed using reference and sensing channels such as in optical fiber sensors. One would expect that reference and sensing channels are not equal due to the changing nature of the sensing channel. In this case, division might provide a better performance compared to difference as it cancels correlated multiplicative noise even if the reference and the sensing channels are not balanced.

## 3. Experimental section

The aim of this section is to present an experimental investigation on the estimation of noise in differential and ratiometric processing in the presence of correlated noise. Since it is focused on the validation of the analytical expressions presented in Section 2, we do not address the problem of how knowledge of correlations can be used to develop new strategies for noise reduction although these are considered in the discussions.

### 3.1. Experimental setup

The analysis of the differential and ratiometric noise was experimentally validated using the differential intensity surface plasmon resonance system described in Fig. 4. The optical system configuration was based on Kretschmann-Raether configuration, in which a plano-convex cylindrical lens was used as a prism. A He-Ne laser was used to produce a linearly polarised light which was focused, using a cylindrical lens, into a line on the gold surface. The system was aligned so as the fan beam is centered at the resonance angle with an angular width of  $\sim 5^\circ$ . The reflected light was collimated by using another cylindrical lens before it was detected by a pixelated camera. The sensing structure that was used to excite SPs was fabricated of a glass substrate ( $n = 1.515$ ) coated with 50 nm of gold by sputtering. The excitation of SPs features a drop in the intensity, as presented by a blue line in Fig. 5, indicating the position of the resonance angle. The horizontal axis of the reflected intensity refers to the angle of incidence which can be calculated using the geometry of the reflected beam, the collimating optics and the pixelated camera.

### 3.2. Experimental validation of differential and ratiometric noise

To validate the theoretical expressions to estimate the differential and ratiometric noise presented in Section 2, a pixelated camera was used to monitor the intensity fluctuations of the SPR curve over time (i.e., collecting a data set of  $R(\theta, t)$ ). This was performed by recording the reflected light for 30 s with a sampling frequency of 10 Hz. Fig. 5 shows an example intensity map, in which the horizontal axis represents the angular information while the vertical axis represents spatial information. A virtual bicell is centered on

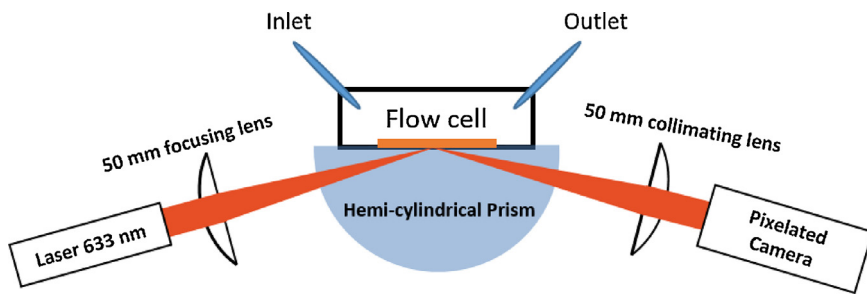


**Fig. 4.** Optical system configuration of the differential intensity surface plasmon resonance system.

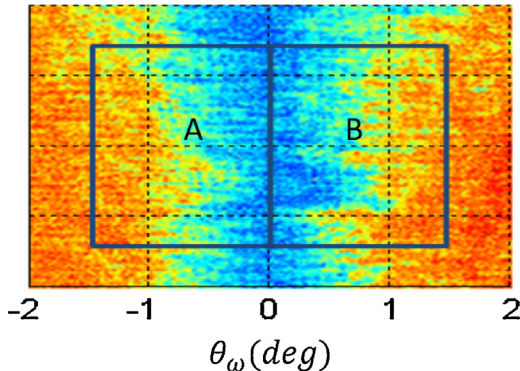


**Fig. 5.** The distribution of the intensity of the reflected beam; spatial information on the vertical axis and angular information on the horizontal domain. The rectangle shows coordinates of the virtual bicell detector that is centred on the resonance angle. (For interpretation of the references to colour in the text, the reader is referred to the web version of the article.)

the resonance angle ( $\theta_\omega = 0$ ), and its width is defined in terms of the angular widths while its height in pixels is  $\pm 100$  pixels in this experiment.  $A$  and  $B$  are used to denote the two channels of the virtual detector.

For each frame, the intensity of the channel ( $A$  or  $B$ ) was calculated by summation of the intensity of the pixels that form the defined area of the bicell. The value obtained represents a data point in the time series that is used to calculate the difference ( $A - B$ ), the sum ( $A + B$ ) and the ratio ( $(A - B)/(A + B)$ ). To test the noise dependence on the angular width, this process was repeated for a set of angular widths starting from  $0.066^\circ$  to  $2.6^\circ$ . For each of these data sets (i.e., 300 samples), the standard deviation (i.e., the noise) and the average value of the signal were calculated as a function of the angular width ( $\theta_w$ ).

In order to verify the theoretical expressions presented in Section 2.2, noise of the difference ( $A - B$ ), the sum ( $A + B$ ) and their ratio ( $(A - B)/(A + B)$ ) were obtained by the following two methods. Noise was calculated from the standard deviation that is directly obtained from the time-varying signals. The results were compared to noise calculated from the primary signals  $A$  and  $B$  using the theoretical expressions: Eqs. (4) and (9) described in Section 2. As mentioned in Section 2.2, Eq. (9) is made suitable to calculate the differential and ratiometric noise in bicell-based SPR systems.

### 3.3. Refractive index stepping

In order to study the effect of the detector balance on the noise of the differential and ratiometric signal, the refractive index of the sample was stepped in increments of 0.5 mRIUs starting from 1.3294 to 1.3344 using series of concentrations of sodium chloride solution (dissolved in  $\text{dH}_2\text{O}$ ) while the reflected light intensity was recorded using the pixelated camera. The recorded frames were

postprocessed to calculate the outputs of the virtual detector  $A$ ,  $B$ ,  $A - B$ ,  $A + B$  and the ratio of difference to sum.

## 4. Results and discussion

For SPR systems in which the bicell detector is used, the outputs ( $A$  and  $B$ ) are processed to obtain  $(A - B)/(A + B)$  that is directly related to the shift in the resonance position as discussed in [1,13]. The noise of the output of the bicell-based SPR  $(A - B)/(A + B)$  can be calculated with the knowledge of the noise in the channels  $A$  and  $B$  and their covariance. In this section, the set of equations described in Section 2 was verified experimentally by comparison to the direct calculation of noise from the standard deviation of the time-varying signals. First, Eq. (1) is used to obtain the noise of the difference and the sum. Second, with the knowledge of the noise of the two signals obtained from the previous step, alongside to their average values and their covariances, the noise of the ratio  $(A - B)/(A + B)$  was calculated using Eq. (9). The use of the previous expressions to calculate the noise of the difference, the sum and the ratio was confirmed experimentally by varying the angular width of the excitation beam and measuring the noise of the components of the virtual bicell detector.

### 4.1. Differential and ratiometric noise

Fig. 6 presents the noise of the difference (Fig. 6(a)) and the sum (Fig. 6(b)) calculated using Eq. (4), similarly these noise values can be found from the standard deviation of the traces of  $(A - B)$  and  $(A + B)$ . The proposed approach can be used for accurate calculation of the noise of the difference and the sum, taking into consideration the effect of the correlated and uncorrelated components of the noise. It is observed from this graph that noise increases with the angular width of the excitation beam due to the increase of the detected optical power, as one would expect. The presence of correlated noise is also observed from Fig. 6. The effect of this component is reduced by the performing the difference while it increases with the summing.

### 4.2. The effect of correlation between the bicell signals

We can see from Fig. 6, how the presence of the correlated components of the noise affect the difference and the sum of the two signals. In time-resolved measurements, the presence of correlated noise is expected to vary during the time course of the experiment, as shown in Fig. 7. The correlation between the signals of the bicell detector is measured after dividing them into small windows of one second. The presence of positive correlation can be attributed to coherent fluctuation in the intensity light source, while the negative correlation can be an indication of angular noise. Angular noise can be described as oscillations or drift in the apparent resonance position due to the laser pointing oscillations or temperature drift. On the other hand, low or no correlation

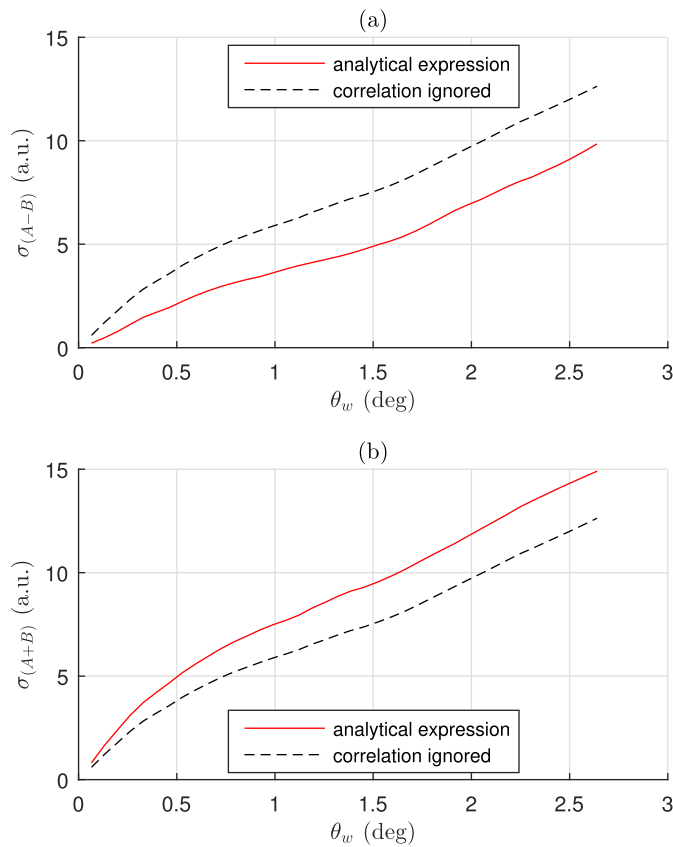


**Fig. 6.** Noise of the difference ( $A - B$ ) and the sum ( $A + B$ ) of the virtual bicell detector signals in (a) and (b) respectively. Noise was calculated from the experimental data  $A - B$  and  $A + B$  over 30 seconds of time-varying signals using mathematical operations on random variables after calculating the variances and covariance of the original signals  $A$  and  $B$ . The dash line represents the case of where the correlation or the covariance between the signals  $A$  and  $B$  is ignored.

is an indication of random noise such as shot or thermal noise. Additionally, correlation is reduced due to factors related to the design of the experimental setup such as speckles in the detected intensity map, the presence of microphonics or mechanical instability. Anticorrelated noise can be removed by using a second order differential or ratiometric processing that can be performed with dual-bicell detector and dual-channel [24] or quadrant photodiode [32] aligned to reference and measurement channels. Suppression of the anticorrelated noise using referenced measurements allows accurate measurement of the dynamics of the resonance position. Furthermore, measurements of correlation in real time can be used to design adaptive noise removal in differential and ratiometric measurements. Additionally, the knowledge of the correlation can provide methods to improve the signal to noise ratio of a system. For instance, we have shown that in structured light microscopy [23] information about similar spatial frequencies is encoded in different extracted signals. The optimum signal to noise can thus be achieved by weighting these contributions appropriately and indeed we show that these optimum weightings are dependent on the correlation between the noise of the different components. While the differential intensity system does not contain much duplicate information, a similar strategy could be implemented by adjusting the weighting of the different parts of the detector. For instance, the region close to the center of the detector does not contribute to a large portion of the detected signal but does contribute to the noise, so weighting the central part less strongly can optimise the signal to noise ratio. Such optimisations require

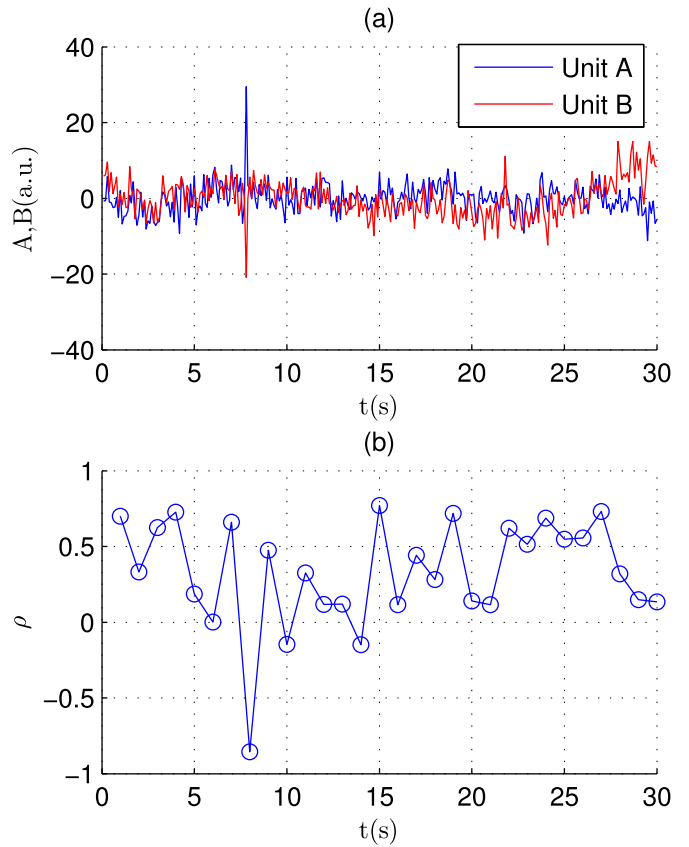


**Fig. 7.** Temporal fluctuation of the correlation ( $\rho$ ) measured over 1 s time windows (b) between the signals of the two units of the virtual bicell detector shown in (a).

a substantial new study which we hope will be the subject of a subsequent publication.

#### 4.3. Noise of normalised differential signals

In order to validate the approximation for variance of the ratio, the noise of the ratio  $(A - B)/(A + B)$  was calculated, for a set of angular widths of the virtual bicell detector, using Eq. (4) and compared to the noise that is directly calculated from the standard deviation of the temporal fluctuations of the ratio  $(A - B)/(A + B)$ . The good agreement between the two methods, presented in Fig. 8, shows that the approximation of the variance of the ratio can be used to obtain the noise of the  $(A - B)/(A + B)$  in systems that use bicell detectors as long as the assumptions stated in Section 2.1 are satisfied. As the denominator  $(A + B)$  is the sum of the bicell detector signals, the condition that the random variable of the denominator takes positive values is always satisfied for the SPR based on bicell detectors. As noticed in Fig. 8, noise of the ratio decreases as the angular width increases; this trend is expected as the noise of the ratio is proportional to the reciprocal of the fourth power of the average power of the reflected light. As will be explained later in this section, the noise of the ratio can be approximated by Eq. (10).

#### 4.4. The effect of the balance of the bicell detector

As we discussed earlier in Section 2.3, when the detector is unbalanced, the random additive noise dominates the ratio  $(A - B)/(A + B)$  (Eq. (14)) even though the correlative multiplicative noise is canceled by performing the division. Since the sensitivity depends on the noise performance, the contribution of the uncorrelated additive noise is expected to affect the detection limit of the system. In this section, we show how the detector unbalance affects

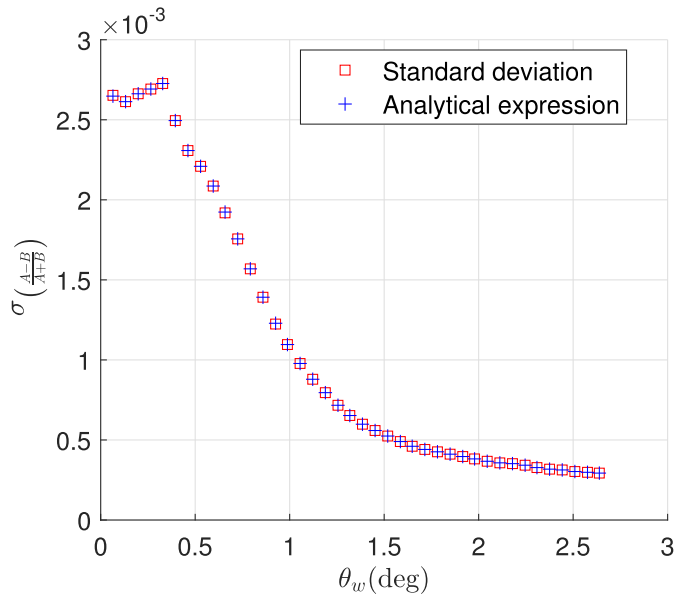


**Fig. 8.** Experimental noise of the ratio  $(A-B)/(A+B)$  obtained from the standard deviation of  $(A-B)/(A+B)$  calculated over 30 seconds (represented by the squares) while the plus sign shows noise calculated using the analytical expression of the noise of the ratio (Eq. (9)) with knowledge of the experimental variances, average values and the covariance of the difference  $(A-B)$  and the sum  $(A+B)$ .

the noise of  $(A-B)/(A+B)$  and the sensitivity (i.e. the detection limit) of bicell SPR systems during experiments.

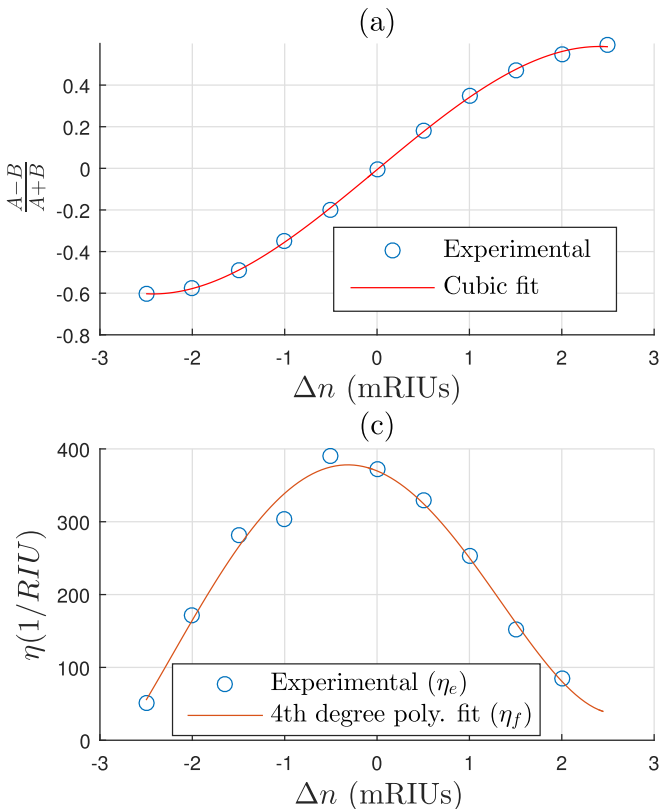
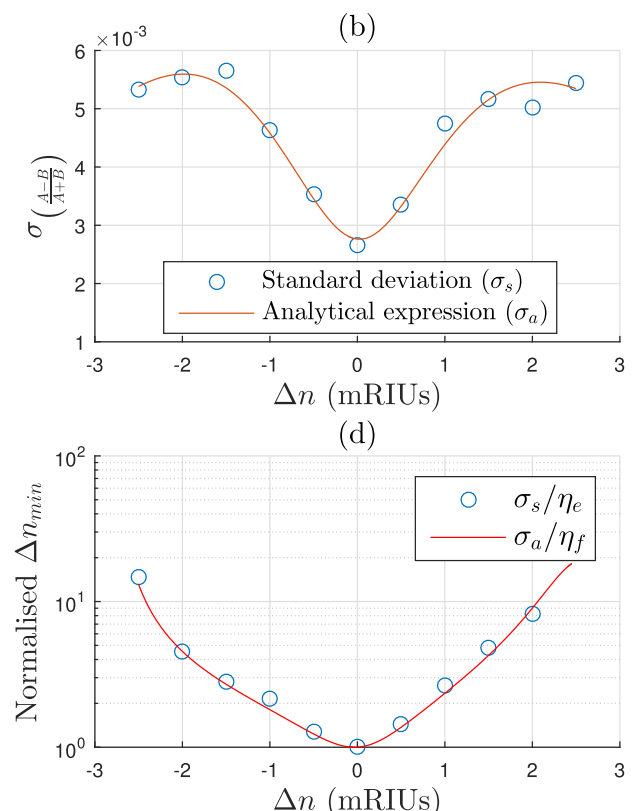


**Fig. 9.** Experimental noise of the DI-SPR increases when the detector is unbalanced due to a shift in the resonance position resulting from the change in the refractive index of the sample. (a) The output of the DI-SPR system for a series of refractive index changes (b) the noise of the output of the DI-SPR: circles present noise calculated from the standard deviation of the ratio while solid line presents noise obtained from Eq. (9) using the experimental mean and the standard deviation of the difference and the sum of the bicell outputs  $A$  and  $B$  and their correlation, all smoothed by fitting to quadratic functions and interpolation (c) the responsivity of the system calculated from  $\Delta[(A-B)/(A+B)]/\Delta n$  and (d) is normalised sensitivity obtained by dividing the noise by the responsivity.

In Fig. 9, we showed how noise and sensitivity changes when the detector is unbalanced. The sensitivity, in this paper, is defined as the minimum detectable refractive index change. Also, responsivity is defined as the change in the system output divided by the change in refractive index ( $\Delta[(A-B)/(A+B)]/\Delta n$ ). Sensitivity depends on both the noise and the responsivity of the system (i.e. it is obtained by dividing the noise by the responsivity of the system). The response of the system  $(A-B)/(A+B)$  to a change in refractive index is shown in Fig. 9(a) fitted to a cubic function while the noise of the ratio is presented in Fig. 9(b). Noise is obtained from the standard deviation that is directly calculated from the traces of the system output,  $(A-B)/(A+B)$ . This is compared to the noise calculated from the analytical expression in Eq. (9). The values of the input parameters ( $\sigma_{(A-B)}$ ,  $\sigma_{(A+B)}$ ,  $\mu_{(A-B)}$ ,  $\mu_{(A+B)}$ ,  $\sigma_A$  and  $\sigma_B$ ) are calculated for a series of refractive index steps, and the obtained data is smoothed by fitting to a quadratic function and then interpolating. Responsivity, presented in Fig. 9(c), is calculated from Fig. 9(a) by finding  $\Delta[(A-B)/(A+B)]/\Delta n$  and the data points are fitted to a 4th degree polynomial function. The sensitivity is calculated from Fig. 9(b) and (c) as shown Fig. 9(d).

As suggested by Eq. (10), noise of the ratio is changed when the detector is unbalanced. When the refractive index of the sample is changed, the SPR curve is shifted from its initial position unbalancing the detector. Fig. 9(b) shows that noise of the ratio  $(A-B)/(A+B)$  increases if the detector is unbalanced by shifting the resonance curve to the left or the right. This trend is also supported by the noise predicted by Eq. (9) showing a good agreement with noise obtained from the standard deviation of the ratio  $(A-B)/(A+B)$ . Not only does the noise increase when the detector is unbalanced, but also the responsivity to change in refractive index decreases as



explained in [13] and shown in Fig. 9(a). As a result of the effect of the two factors, the sensitivity of system decreases, as shown in Fig. 9(d). For an angular range of  $0.7^\circ$ , the sensitivity drops by an order of magnitude if the refractive index of the sample changes by 2.5 mRIU. Similarly, the dynamic range drops when the detector is unbalanced. However, the system is highly tuneable as discussed in [13] and a tradeoff between the sensitivity and the dynamic range can be obtained by the selecting an appropriate angular range [13].

We conclude from the effect of the detector balance that the system sensitivity does not change significantly when measurements fall within a narrow range of refractive index change (for example  $\pm 1$  mRIU). In practice, this is equivalent to detection of low concentration of biomolecules. However, for measurements that are made over a wider range (i.e. high concentration of biomolecules), the effect of the detector unbalance needs to be compensated. For instance, adaptive detector balance can be implemented using mechanical methods (e.g. angle scanning) or non-mechanical methods (e.g. pixelated detector [33]). It should be pointed out that in the present measurements the noise values were relatively large because the detected power in the pixelated camera was low. Noise can be reduced significantly by increasing the detected power as suggested by Eq. (10) and reported previously by [1].

## 5. Conclusions

Sensitive detection of small signals such as binding of small biomolecules requires developing instrumentation with high signal to noise ratio. In many cases, the design process involves the use of differential or ratiometric methods to cancel the common-mode fluctuations. The evaluation of the performance of these methods is often qualitative, which limits a complete characterisation of system sensitivity. This paper proposes formulations for evaluating noise and signal to noise ratio in differential and ratiometric signal processing systems in the presence of noise with different degrees of correlation. Calculation of noise in differential intensity surface plasmon resonance system, which uses bicell photodetection, is presented as an example where these formulas can be used to provide better understanding of the performance of the sensing system. We showed that these formulations can be used to estimate the noise and the noise to signal ratio of differential or ratiometric measurements. Performing either division or difference on the signals of the bicell detector suppress the correlated noise components under the condition that the detector is balanced. Correlated multiplicative noise is canceled by performing the division even if the detector is unbalanced while the random noise increases, which can be reduced by averaging if measurements are performed over a suitable timescale. Noise of the differential intensity SPR increases and the responsivity of the system drops when the detector is unbalanced. During experiments, the detector can become unbalanced due to the shift in the resonance position in response to changes in refractive index of the sample. As a result the sensitivity of the system decreases, in particular, if the measurements are performed over a wide range of refractive index change. The effect of the detector unbalance can be compensated by performing adaptive detector balance during the experiment.

## Acknowledgements

This work was supported by the Engineering and Physical Sciences Research Council [grant numbers EP/G005184/1, EP/M50810X/1]; and the University of Nottingham.

## References

- [1] N. Tao, S. Boussaad, W. Huang, R. Arechabaleta, J. D'Agnese, High resolution surface plasmon resonance spectroscopy, *Rev. Sci. Instrum.* 70 (12) (1999) 4656–4660.
- [2] H. Raether, *Surface Plasmons on Smooth Surfaces*, Springer, 1988.
- [3] M.G. Somekh, S. Liu, T.S. Velinov, C.W. See, High-resolution scanning surface-plasmon microscopy, *Appl. Opt.* 39 (34) (2000) 6279–6287.
- [4] J. Homola, Surface plasmon resonance sensors for detection of chemical and biological species, *Chem. Rev.* 108 (2) (2008) 462–493.
- [5] A. Dahlin, B. Dielacher, P. Rajendran, K. Sugihara, T. Sannomiya, M. Zenobi-Wong, J. Vörös, Electrochemical plasmonic sensors, *Anal. Bioanal. Chem.* 402 (5) (2012) 1773–1784.
- [6] X. Fan, I.M. White, S.I. Shopova, H. Zhu, J.D. Suter, Y. Sun, Sensitive optical biosensors for unlabeled targets: a review, *Anal. Chim. Acta* 620 (1) (2008) 8–26.
- [7] J. Homola, S.S. Yee, G. Gauglitz, Surface plasmon resonance sensors: review, *Sens. Actuators B: Chem.* 54 (1) (1999) 3–15.
- [8] B.P. Nelson, T.E. Grimsrud, M.R. Liles, R.M. Goodman, R.M. Corn, Surface plasmon resonance imaging measurements of DNA and RNA hybridization adsorption onto DNA microarrays, *Anal. Chem.* 73 (1) (2001) 1–7.
- [9] Y. Huang, H. Ho, S. Wu, S. Kong, Detecting phase shifts in surface plasmon resonance: a review, *Adv. Opt. Technol.* (2012).
- [10] K. Johansen, R. Stålborg, I. Lundström, B. Liedberg, Surface plasmon resonance: instrumental resolution using photo diode arrays, *Meas. Sci. Technol.* 11 (11) (2000) 1630.
- [11] G.G. Nenninger, M. Pilariuk, J. Homola, Data analysis for optical sensors based on spectroscopy of surface plasmons, *Meas. Sci. Technol.* 13 (12) (2002) 2038.
- [12] O.R. Bolduc, L.S. Live, J.F. Masson, High-resolution surface plasmon resonance sensors based on a dove prism, *Talanta* 77 (5) (2009) 1680–1687.
- [13] S.A. Abayzeed, R.J. Smith, K.F. Webb, M.G. Somekh, C.W. See, Responsivity of the differential-intensity surface plasmon resonance instrument, *Sens. Actuators B: Chem.* 235 (2016) 627–635.
- [14] A. Stuard, J.K. Ord, *Kendall's Advanced Theory of Statistics, Distribution Theory*, vol. 1, 1994.
- [15] F. Frishman, On the arithmetic means and variances of products and ratios of random variables, in: *A Modern Course on Statistical Distributions in Scientific Work*, Springer, 1975, pp. 401–406.
- [16] A. Blanchard-Dionne, L. Guyot, S. Patkovsky, R. Gordon, M. Meunier, Intensity based surface plasmon resonance sensor using a nanohole rectangular array, *Opt. Express* 19 (16) (2011) 15041–15046.
- [17] X. Wang, M. Jefferson, P.C. Hobbs, W.P. Risk, B.E. Feller, R.D. Miller, A. Knoesen, Shot-noise limited detection for surface plasmon sensing, *Opt. Express* 19 (1) (2011) 107–117.
- [18] R.C. Posner, B. Lawrie, Plasmonic trace sensing below the photon shot noise limit, *ACS Photonics* 3 (1) (2015) 8–13.
- [19] Y.C. Li, Y.F. Chang, L. Su, C. Chou, Differential-phase surface plasmon resonance biosensor, *Anal. Chem.* 80 (14) (2008) 5590–5595.
- [20] S. Wu, H. Ho, W. Law, C. Lin, S. Kong, Highly sensitive differential phase-sensitive surface plasmon resonance biosensor based on the mach-zehnder configuration, *Opt. Lett.* 29 (20) (2004) 2378–2380.
- [21] M. Pilariuk, J. Homola, Surface plasmon resonance (SPR) sensors: approaching their limits? *Opt. Express* 17 (19) (2009) 16505–16517.
- [22] A.V. Kabashin, S. Patkovsky, A.N. Grigorenko, Phase and amplitude sensitivities in surface plasmon resonance bio and chemical sensing, *Opt. Express* 17 (23) (2009) 21191–21204.
- [23] M.G. Somekh, K. Hsu, M.C. Pittet, Effect of processing strategies on the stochastic transfer function in structured illumination microscopy, *J. Opt. Soc. Am. A* 28 (9) (2011) 1925–1934.
- [24] Z. Wang, D.J. Bornhop, Dual-capillary backscatter interferometry for high-sensitivity nanoliter-volume refractive index detection with density gradient compensation, *Anal. Chem.* 77 (24) (2005) 7872–7877.
- [25] S.B. Pal, A. Halder, B. Roy, A. Banerjee, Measurement of probe displacement to the thermal resolution limit in photonic force microscopy using a miniature quadrant photodetector, *Rev. Sci. Instrum.* 83 (2) (2012) 023108.
- [26] Y. Guan, X. Shan, F. Zhang, S. Wang, H.Y. Chen, N. Tao, Kinetics of small molecule interactions with membrane proteins in single cells measured with mechanical amplification, *Sci. Adv.* 1 (9) (2015) e1500633.
- [27] S. Achamfu-Yeboah, R. Light, S. Sharples, Optical detection of ultrasound from optically rough surfaces using a custom CMOS sensor *Journal of Physics: Conference Series*, vol. 581, IOP Publishing, 2015, pp. 012009.
- [28] J. Broder, A. Majumder, E. Porter, G. Srinivasamoorthy, C. Keith, J. Lauderdale, A. Sornborger, Estimating weak ratiometric signals in imaging data. I. Dual-channel data, *J. Opt. Soc. Am. A* 24 (9) (2007) 2921–2931.
- [29] J. Wang, R.J. Smith, R.A. Light, J.L. Richens, J. Zhang, P. O'Shea, C. See, M.G. Somekh, Highly sensitive multipoint real-time kinetic detection of surface plasmon bioanalytes with custom CMOS cameras, *Biosens. Bioelectron.* 58 (2014) 157–164.
- [30] H. Seltman, Approximations for mean and variance of a ratio, <http://www.stat.cmu.edu/hselzman/files/ratio.pdf> (accessed 20.04.17).
- [31] E.S. Lee, R.N. Forthofer, *Analyzing Complex Survey Data*, vol. 71, Sage Publications, 2005.
- [32] H. Zhang, S. Boussaad, N. Tao, High-performance differential surface plasmon resonance sensor using quadrant cell photodetector, *Rev. Sci. Instrum.* 74 (1) (2003) 150–153.

- [33] J. Rhee, D. Wang, N. Tao, Y. Joo, CMOS image sensor array for surface plasmon resonance spectroscopy, in: *Electronic Imaging 2004, International Society for Optics and Photonics*, 2004, pp. 34–41.

## Biographies

**Dr. Sidahmed Abayzeed** received BEng (Hons) in Biomedical Engineering from Sudan University of Science and Technology, Khartoum, Sudan. He obtained MSc in Bioengineering (2011) and PhD in Electrical and Electronic Engineering (2016) both from the University of Nottingham, UK. In 2016, he was awarded EPSRC Doctoral Prize at the University of Nottingham – a two-year postdoctoral fellowship to develop plasmonic-based impedance micro-spectroscopy of living cells.

**Dr. Richard J. Smith** completed his MEng in electronic and electrical engineering in 2002, and went on to obtain an PhD on combining optical microscopy and signal processing techniques to expand the measurement capabilities of optical microscopes in 2006, both from the University of Nottingham. He is currently assistant professor in Optical and Electronic Engineering, at the University of Nottingham, with research interests in plasmonics, and nano structures/devices for use in high frequency laser ultrasonics.

**Dr. Chung W. See** graduated in Electronic and Electrical Engineering from University College London in 1981, and received his PhD in 1986, also from UCL. His PhD and

Post-Doctoral research concerned high resolution, ultra-sensitive optical systems for imaging and metrology. From 1988 to 1992, CWS worked as a Senior Research Engineer at Rank Taylor Hobson Ltd, Leicester. His primary responsibility was to develop various optical metrology systems for texture, and form measurements. CWS joined the School of Electrical and Electronic Engineering, University of Nottingham in October 1992 as a Lecturer, and was appointed a Senior Lecturer in 2001. His research interests concern optical imaging systems, including super-resolution techniques and ultra-sensitive imaging using surface plasmon resonance.

**Prof. Michael G. Somekh** took his first degree from Oxford University in Metallurgy and Materials Science. He then completed his PhD in Microwave Electronics from Department of Physics, University of Lancaster in 1981. He then returned to Oxford to work on contrast mechanisms in Acoustic Microscopy first as a research associate then as an EPSRC Research Fellow. He then joined University College London as lecturer and Director of the Wolfson Unit for micro-NDE. In 1989 he joined the University of Nottingham as Senior Lecturer and was promoted to Reader (1992) and Professor of Optical Engineering (1994). His research interests are novel microscopy, imaging sensors and laser ultrasonics. He is Chair Professor in Biophotonics at Hong Kong Polytechnic University. Mike was elected to the Royal Academy of Engineering (the UK engineering Academy) in 2012 in recognition of his interdisciplinary work. In addition to his post at PolyU he is an honorary professor at the University of Nottingham and Zhejiang University, Hangzhou.